J IRAN CHEM SOC (2015) 12:1235–1243
DOI 10.1007/s13738-015-0587-y

ORIGINAL PAPER

Selective extraction and sensitive determination of mercury (II) ions by flame atomic absorption spectrometry after preconcentration on an ion-imprinted polymer-coated maghemite nanoparticles

Tayyebeh Madrakian · Borhan Zadpour · Mazaher Ahmadi · Abbas Afkhami

Received: 21 July 2014 / Accepted: 2 January 2015 / Published online: 9 January 2015

Abstract An ion-imprinted polymer-coated maghemite nanoparticle adsorbent for selective extraction of Hg(II) ion was synthesized. The polymerization was carried out by the new mercaptoethylamino monomer as the functional monomer, ethylene glycol dimethacrylate as the crosslinking agent and ammonium persulfate as the initiator in the presence of Hg(II) ions as the template. The synthesized nanoparticles were characterized using FT-IR, XRD and TEM analysis. The effects of various factors that may affect the solid-phase extraction of Hg(II) (i.e. pH, adsorbent dosage, contact time) and the preconcentration factor (i.e. initial sample volume, type and volume of the desorbing solvent) were optimized using one-at-a-time method. The maximum adsorption capacity was obtained as 72.8 mg g^{-1}. Compared with the non-imprinted polymer-coated nanoparticles, the synthesized ion-imprinted polymer-coated nanoparticles had higher selectivity for Hg(II). The detection limit was found to be 4.1 μg L^{-1} for an initial sample volume of 200.0 mL using flame atomic absorption spectrometry. The developed method was successfully applied to the determination of trace amounts of mercury in tap water and wastewater samples.

Keywords Maghemite nanoparticles · Solid-phase extraction · Mercury ion · Ion-imprinted polymer · Flame atomic absorption spectrometry

T. Madrakian (✉) · B. Zadpour · M. Ahmadi · A. Afkhami
Faculty of Chemistry, Bu-Ali Sina University, Hamedan, Iran
e-mail: madrakian@basu.ac.ir; madrakian@gmail.com

Introduction

Toxicity and widespread usage of various harmful heavy metal ions and their uncontrollable release into the environment have attracted great attention in the recent years, worldwide. Mercury (II) is a widely distributed environmental pollutant in aqueous environments and its toxicity to humans and animals even at low concentrations is well known. Mercury (II) is included in all the lists of priority pollutants as a result, and the different regulations and guidelines have been developed for monitoring its levels in water and sediments [1].

To determine trace metals in aquatic environments by instrumental analysis a separation and preconcentration technique is frequently required, which is because of low concentration of trace metal ions and presence of interferences [2–5]. Many sample pretreatment methods (e.g. solvent extraction, cloud point extraction, solid-phase extraction, membrane filtration, electrodeposition, flotation, coprecipitation and ion exchange) have been developed for the preconcentration of trace metals from natural waters [4–13]. Among these techniques, solid-phase extraction (SPE) procedures are considered superior to other procedures for their simplicity, consumption of small volumes of organic solvent and ability to achieve a higher enrichment factor.

New SPE sorbents have recently appeared as alternatives to conventional solid-phase extraction sorbents with the aim of achieving a more selective preconcentration of the target analytes. Molecular imprinting has become an established technique for preparing robust molecular recognition elements for a wide variety of target molecules [14, 15]. Molecularly imprinting polymers (MIPs) have been investigated as highly selective sorbents for SPE to concentrate and clean up samples prior to analysis. MIPs,

involving the formation of cavities in synthetic polymer for a template analyte, are useful for selective extraction. This analytical method is a rapidly developing technique for the preparation of polymeric materials that are capable of high molecular recognition [16–20]. Scientists always try to prepare imprinting polymers with high affinity toward the template compounds. For this purpose, the type of monomers and polymerization are designed for better selectivity. A particularly promising application of ion-imprinted polymer (similar to MIPs) is the solid-phase extractive preconcentration and/or separation from other coexisting ions or complex matrices [21–23].

In this work, an ion-imprinted polymer adsorbent is introduced as a solid phase for the selective extraction of Hg(II) from wastewater samples. Then, the concentration of Hg(II) in the extract solution was determined using flame atomic absorption spectrometry. It should be noticed that several solid supports, such as chelating resins [24], modified silica [25], modified clay [26], alumina [27] and ion exchange resins have also been used for the preconcentration of mercury (II) ion or its other forms. However, the present method is more rapid, simple and sensitive, compared with previous ones. The developed procedure was successfully applied to the determination of Hg(II) ions in wastewater samples.

Experimental

Reagents and apparatus

All the used chemicals were of analytical reagent grade or the highest purity available and were purchased from Merck Company (Darmstadt, Germany). Aqueous solutions of chemicals were prepared with double distilled water (DDW). The stock solutions of Hg(II) ion were prepared from its nitrates salt as 1,000 mg L^{-1}. Working solutions, as per the experimental requirements, were freshly prepared from the stock solution for each experimental run. Britton–Robinson universal buffer was used for pH adjustment of the working solutions.

A Metrohm model 713 (Herisau, Switzerland) pH-meter was used for pH measurements. The concentration of the metal ion was determined by atomic absorption spectrometry using an Aurora model Spect AI 1200 apparatus. The instrumental settings of the manufacturer were followed. Transmission electron microscopy (TEM) involved use of TEM, Philips, CM10, 100 kV transmission electron microscope. X-ray diffraction (XRD) measurement involved use of an X-ray diffractometer (XRD) (38066 Riva, d/G.Via M. Misone, 11/D (TN) Italy) at ambient temperature with Cu K-alpha (Cu K_{α}) radiation. Infra-red (IR) spectra were recorded with use of a Fourier transform infrared spectrometer (FT-IR, Perkin Elmer, spectrum 100).

Preparation of maghemite nanoparticles (MNPs) and SiO_2-coated MNPs (SCMNPs)

Maghemite nanoparticles (MNPs) were prepared according to the previously reported procedure [28]. Then, synthesized MNPs were coated with a layer of SiO_2 according to the following procedure: typically, 0.5 g of MNPs was dispersed in 60.0 mL ethanol and 10 mL of DDW water by sonication for 15 min, followed by the addition of 1.0 mL ammonium hydroxide (25 %) and 3.0 mL tetraethoxysilane (TEOS) sequentially. The mixture was reacted for 12 h at room temperature under continuous stirring. The resultant product (SiO_2-coated MNPs, SCMNPs) was collected by an external magnetic field, and rinsed six times with ethanol and DDW, respectively. Finally, the SCMNPs obtained were dried under vacuum at 60 °C for 3 h.

Preparation of Hg(II)-imprinted polymer-coated maghemite nanoparticles (HgIPMNPs)

The mercaptoethylamino monomer was synthesized according to a previously reported procedure with some modifications [14]. Briefly, the mercaptoethylamino monomer was synthesized by slow addition of 1 g (0.01 mol) maleic anhydride to the solution of 1.7 g (0.015 mol) cysteamine hydrochloride in 20 mL DDW. The solution was heated at 120 °C for 1 h, until all the water was removed and cysteamine reacted with the maleic anhydride through ring-opening reaction (Scheme 1a).

To prepare HgIPMNPs, the mercaptoethylamino monomer (functional monomer) was polymerized in the presence of SCMNPs (0.5 g) and ammonium persulfate (0.1 g, as the initiator), ethylene glycol dimethacrylate (20 μL, as the cross-linking monomer) and Hg(II) (0.01 g, as the template) in 30 mL DDW at 85 °C for 12 h (Scheme 1b). The product was separated using an external magnet and washed with methanol to remove unreacted reagents and then washed overnight with a mixture of thiourea (0.5 mol L^{-1})/nitric acid (0.05 mol L^{-1}) aqueous solution (1:1, v/v) to remove the template. Finally, the product was washed with DDW to neutral pH and the resulting particles were dried under vacuum for 12 h. The NIP nanoparticles were also synthesized by the same procedure, without addition of the template.

Removal and preconcentration experiments

To a 20.0 mL sample solution containing Hg(II) and 10.0 mL Britton–Robinson buffer solution of pH 5.5, 0.04 g of HgIPMNPs was added. The solution was shaken at room

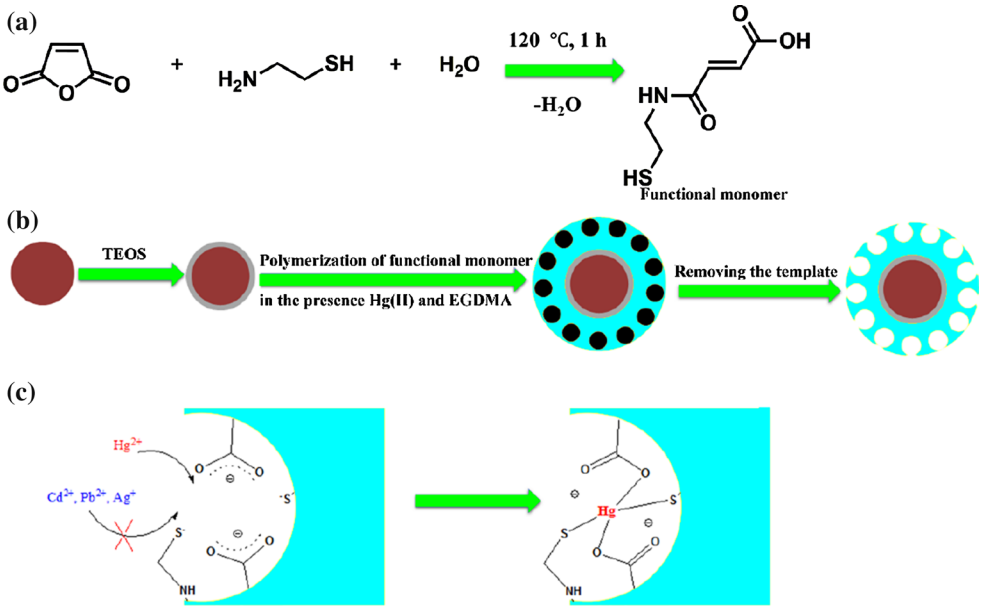

Scheme 1 Schematic representations of **a** functional monomer synthesis, **b** HgIPMNPs nanoparticles synthesis and **c** selectivity origin of IIP cavity

temperature for 60.0 min. Subsequently, the Hg(II)-loaded HgIPMNPs were separated from the mixture with a permanent hand-held magnet within 60 s. The residual amount of the metal ion in solution was determined using atomic absorption spectrometer at 253.7 nm. The percent adsorption, i.e., the metal ion removal efficiency, was determined using the following equation:

$$\%\ \text{Removal efficiency} = \left[\frac{C_0 - C_t}{C_0}\right] \times 100 \qquad (1)$$

where C_0 and C_t represent the initial and final (after adsorption) concentrations of the Hg(II) in mg L^{-1}, respectively. Also, all the experiments were performed at room temperature.

Preconcentration studies for the determination of trace amounts of Hg(II) were performed by the addition of 200.0 mL of solution containing 20.0–1,000.0 μg L^{-1} of Hg(II) and 150 mL of Britton–Robinson buffer of pH 5.5 to 0.04 g of HgIPMNPs and the solution was stirred for 60 min. The concentration of Hg(II) decreased with time due to adsorption by the HgIPMNPs. The Hg(II)-loaded nanoparticles were separated with magnetic decantation and desorption was performed with 2.0 mL of a 1:1 (v/v) mixture of thiourea (0.5 mol L^{-1})/nitric acid (0.05 mol L^{-1}) aqueous solution. The concentration of Hg(II) in the resulting solution was measured using atomic absorption spectrometer at 253.7 nm.

Preparation of natural and sewage water samples

The KWC company wastewater (collected from KWC Company, Arak, Iran), and Radiator manufacturing wastewater (collected from Arak, Iran), and tap water (collected from Hamedan, Iran) were immediately filtered through Millipore cellulose membrane filter (0.45 μm pore size), acidified to pH 2.0 with HNO_3, and stored in pre-cleaned polyethylene bottles. After that, pH of the sample was adjusted at 5.5 and the SPE procedure was carried out.

Results and discussion

Characterization of the adsorbents

The FT-IR spectra of the products, in each step of the HgIPMNPs synthesis, were recorded to verify the formation of the expected products. The related spectra are shown in Fig. 1. The characteristic absorption band of Fe–O in MNPs (around 634 cm^{-1}) was observed in Fig. 1a. A peak at about 1,054 cm^{-1} in Fig. 1b is attributed to Si–O in SiO_2. In Fig. 1c the bands around 1,168, 1,610, 1,719, 2,595 and 3,031 cm^{-1}, observed in synthesized monomer can be attributed to the presence of C–N, C=C, C=O, S–H, and =CH groups, respectively. Two new absorption peaks at about 1,700 and 1,160 cm^{-1} in Fig. 1d are assigned to C=O and C–N bands in the polymer-coated final product (HgIPMNPs) [29, 30]. Based on the above results, it can be concluded that the fabrication procedure (Scheme 1b) was successfully performed.

The XRD pattern (Fig. 2) shows diffraction peaks that are indexed to (2 2 0), (3 1 1), (4 0 0), (4 2 2), (5 1 1), (4 4 0), (6 2 0) and (5 5 3) reflection characteristics of the cubic spinel phase of maghemite (JCPDS powder diffraction data file no. 39-1346), revealing that the resultant nanoparticles were mostly γ-Fe_2O_3. The crystallite size was obtained

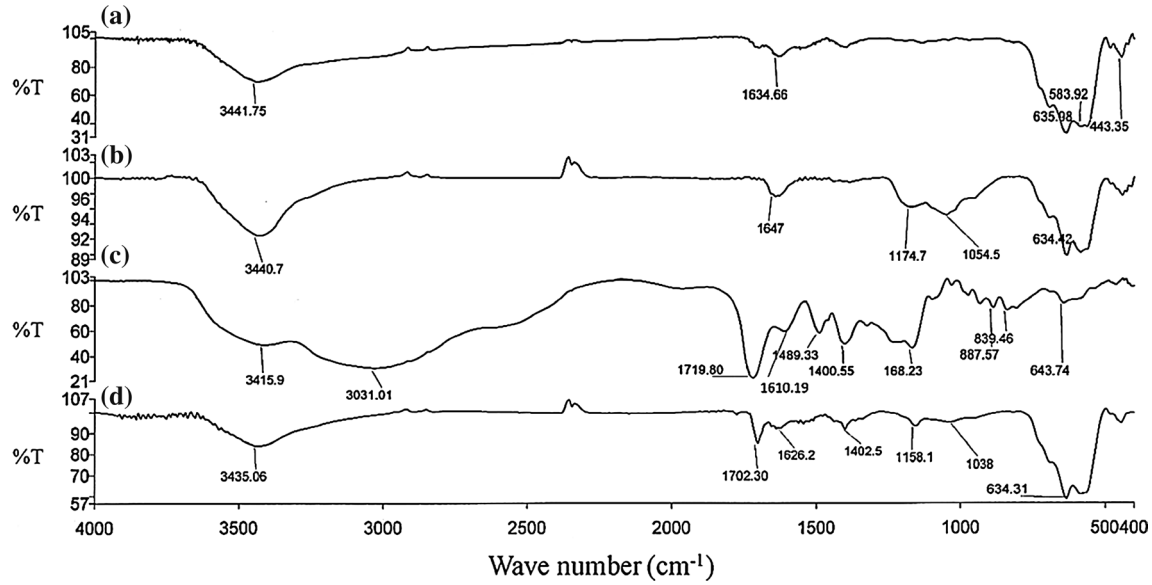

Fig. 1 FT-IR spectra of **a** MNPs, **b** SCMNPs, **c** mercaptoethylamino monomer and **d** HgIPMNPs

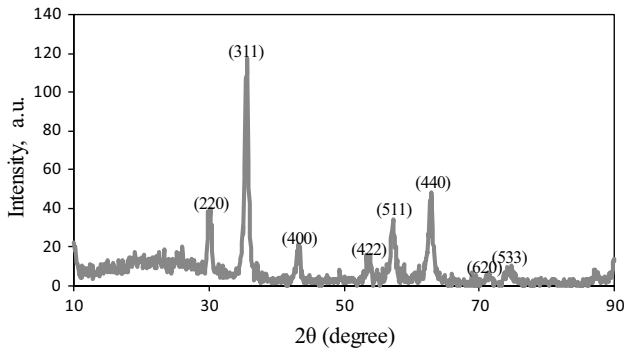

Fig. 2 XRD pattern of the HgIPMNPs nanoparticles

around 11.3 nm from the XRD pattern according to Scherrer equation [28].

TEM revealed the diameters of the MNPs as almost 15–25 nm (Fig. 3a) for a generally homogeneous size and the edges in Fig. 3b shows the immobilization of the core–shell layer in final product.

Point of zero charge (pH_{PZC}) of the adsorbent

The pH_{PZC} of the HgIPMNPs was determined in degassed 0.01 mol L^{-1} $NaNO_3$ solution at 20 °C. Aliquots of 30 mL 0.01 mol L^{-1} $NaNO_3$ were mixed with 30 mg HgIPMNPs in several beakers. The initial pH of the solutions was adjusted at 3.0, 4.0, 5.0, 6.0, 7.0, 8.0, 9.0 and 10.0 using 0.01 mol L^{-1} of HNO_3 and/or NaOH solutions as appropriate. The initial pHs of the solutions were recorded, and the beakers were covered with parafilm and shaken for 24 h. The final pH values were recorded and the differences between the initial and the final pH (the so-called ΔpH) of the solutions were plotted against their initial pH values. The pH_{PZC} corresponds to the pH where ΔpH = 0 [14]. pH_{PZC} for

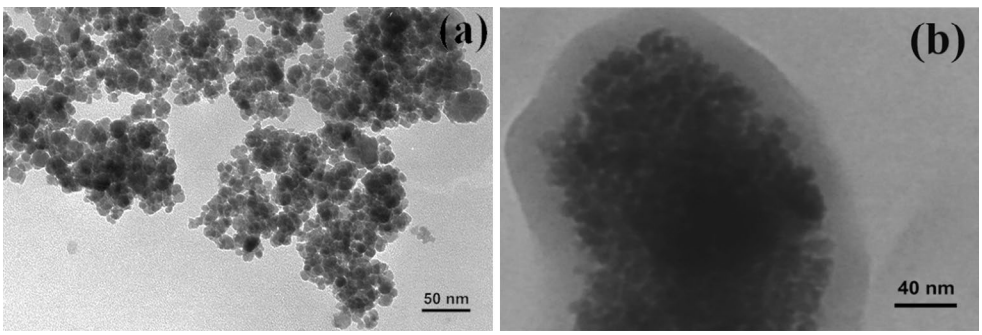

Fig. 3 Transmission electron microscopy image of **a** MNPs and **b** HgIPMNPs nanoparticles

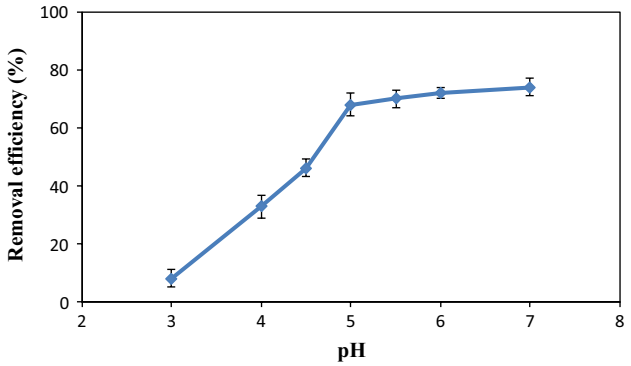

Fig. 4 Effect of pH on the adsorption of Hg(II). Condition: adsorbent, 0.01 g; initial concentration of metal ion, 10.0 mg L^{-1}; volume of metal ion solution, 20.0 mL; time, 30.0 min; at 298 K

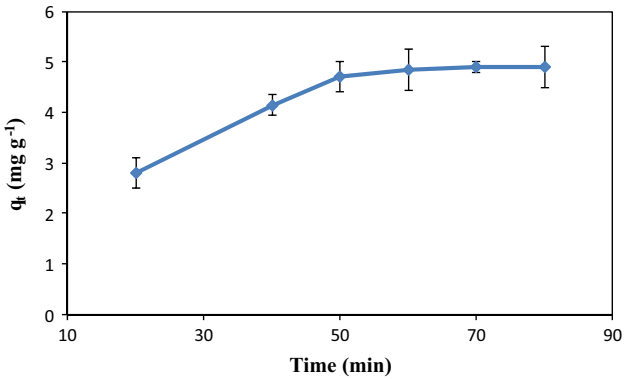

Fig. 5 Effect of time on the adsorption of Hg(II); adsorbent: 0.04 g, initial concentration of the metal ion: 10.0 mg L^{-1}, volume of solution: 20.0 mL, pH: 5.5, at 298 K

HgIPMNPs was determined using the above procedure and was obtained as 4.2.

Adsorption properties of the HgIPMNPs

Effect of pH

One of the important factors affecting the removal of cations from aqueous solutions is the pH of the solution. The dependence of metal sorption on pH is related to both the metal chemistry in the solution and the ionization state of the functional groups of the sorbent which affects the availability of binding sites.

To evaluate the influence of pH on the adsorption of Hg(II) ion, the experiments were carried out within the pH range of 3.0–7.0. A 0.01 g sample of adsorbent was suspended in 20 mL solution of 10.0 mg L^{-1} Hg(II) at several pH values (3.0, 4.0, 4.5, 5.0, 5.5, 6.0 and 7.0), using Britton–Robinson universal buffer for pH adjustment, and removal of the metal ion was investigated. The results are shown in Fig. 4. The removal efficiency increased with pH in the range 3.0–5.0 but remained nearly constant at pHs higher than 5.0.

The observed dependence of removal efficiency on pH may be attributed to the changes in the surface of the adsorbents with pH, which was consistent with the pH-dependent zeta-potential of HgIPMNPs. The pH of zero point charge (pH_{pzc}) was found to be 4.2. At pH < pH_{pzc}, the surface of the adsorbents is positively (or neutrally) charged and therefore adsorption of mercury ion at the adsorbent decreases. By increasing the pH of the solution, the carboxylic acid and thiol functional groups turn into their corresponding anions and the adsorption increases gradually up to pH > pHpzc. After that, functional groups turn completely into their corresponding anions, with almost no change in adsorption. Considering that the metal ion precipitates as hydroxide at higher pHs, the pH 5.5 was chosen for further experiments. The probable adsorption mechanism is that the metal ions are mainly interacted with the adsorbent by chelation between the cation and the carboxylate and thiolate anions (Scheme 1c) [31].

Furthermore, we studied the dependence of the adsorption of cations on the amount of modified nanoparticles at room temperature and at pH 5.5 by varying the adsorbent amount from 0.01 to 0.05 g in contact with 20.0 mL solution of 10 mg L^{-1} Hg(II) cations. The suspension was then stirred for 30.0 min. After magnetically filtering, the supernatant was analyzed for the remaining cations. The results showed that the percentage removal of cation increased by increasing the amount of adsorbent due to the greater availability of the adsorbent. The adsorption reached a maximum with 0.04 g of adsorbent the maximum percentage removal was about 98 %.

Effect of contact time and adsorption kinetic

Figure 5 shows the effects of contact time on the adsorption of the Hg(II) ions. The metal ion adsorption process rapidly reached equilibrium at about 60.0 min. In fact, 95 % of the metal ion became adsorbed at about 50.0 min. To ensure the equilibrium achievements, we used shaking for 60.0 min for all further experiments. The adsorption kinetics of Hg(II) ions with HgIPMNPs was investigated by pseudo-first-order and pseudo-second-order kinetic models, Eqs. (2) and (3), respectively [32].

Pseudo-first order model:

$$\ln(q_e - q_t) = \ln q_e - k_1 t. \quad (2)$$

Pseudo-second-order model:

$$\frac{t}{q_t} = \frac{1}{k_2 q_e^2} + \frac{1}{q_e} t \quad (3)$$

Table 1 Values of the parameters obtained by different kinetic models

Pseudo-first order				Pseudo-second order			
$q_{e,cal}$ (mg g^{-1})	$q_{e,exp}$ (mg g^{-1})	k_1 (min^{-1})	R^2	$q_{e,exp}$ (mg g^{-1})	$q_{e,cal}$ (mg g^{-1})	k_2 (g mg^{-1} min^{-1})	R^2
6.62	4.95	0.038	0.991	4.95	5.17	0.022	0.994

where q_t (mg g^{-1}) is the amount of Hg(II) became adsorbed at time t (min); q_e (mg g^{-1}) is the amount of adsorbed ion at equilibrium; and k_1 (min^{-1}) and k_2 (g mg^{-1} min^{-1}) are the kinetic rate constants for the pseudo-first order and the pseudo-second-order models, respectively. The kinetic adsorption data were fitted to Eqs. (2) and (3), and the calculated results are presented in Table 1. The correlation coefficient (R^2) for the pseudo-second-order adsorption model was higher than that for the pseudo-first-order model. Therefore, the adsorption data are well represented by the pseudo-second order kinetic model.

This result was expected because usually the exchange processes are more rapid and mainly diffusion controlled, whereas those with a chelating exchanger are slower and are controlled by a second-order chemical reaction. The sorbent, HgIPMNPs, which has chelating functional groups on its surface (Scheme 1c), most probably behaves as a chelating exchanger. Therefore, the complexation chemical reaction is expected in the adsorption processes [33] and the rate-limiting step of the adsorption was dominated by a chemical adsorption process [34].

Adsorption isotherm

The capacity of the adsorbent is an important factor that determines how much sorbent is required to quantitatively remove a specific amount of the metal ion from the solution. For measuring the adsorption capacity of HgIPMNPs, the absorbent was added into Hg(II) solutions at various concentrations, and the suspensions were stirred at room temperature, followed by magnetic removal of the absorbent. An adsorption isotherm describes the fraction of the sorbate molecules that are partitioned between the liquid and the solid phase at equilibrium. Adsorption of the metal ion by HgIPMNPs and NIP nanoparticles was modeled using Freundlich [35] and Langmuir [36] adsorption isotherm models. The remained Hg(II) in the supernatants was measured using flame atomic absorption spectrometer, and the results were used to plot the isothermal adsorption curves as shown in Fig. 6. The equilibrium adsorption data were fitted to Langmuir and Freundlich isotherm models by linear regression. The resulting parameters are summarized in Table 2.

The higher correlation coefficient obtained for the Langmuir model ($R^2 > 0.99$) indicates that the experimental data are better fitted into this model, and adsorption of Hg(II) on HgIPMNPs is more compatible with Langmuir assumptions,

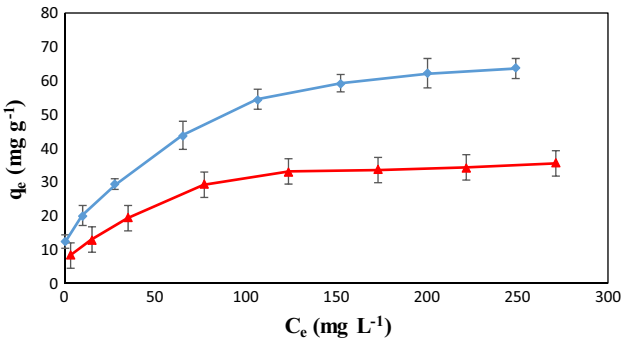

Fig. 6 Isothermal adsorption curves of Hg(II) on HgIPMNPs (*filled diamond*) and on NIP nanoparticles (*filled triangle*)

i.e., adsorption takes place at specific homogeneous sites within the adsorbent. The Langmuir model is based on the physical hypothesis that the maximum adsorption capacity consists of a monolayer adsorption, that there is no interaction between adsorbed molecules, and that the adsorption energy is distributed homogeneously over the entire coverage surface. This sorption model serves to estimate the maximum uptake values where they cannot be reached in the experiments. According to the results (Table 2), the maximum amount of Hg(II) that can be adsorbed by HgIPMNPs was found to be 72.8 mg g^{-1} at pH 5.5. The relatively high adsorption capacity of HgIPMNPs shows that the adsorption of Hg(II) ions takes place at a large number of specific homogeneous sites within the adsorbent (specific cavities of the MIP), besides non-specific interactions which are approximately identical for both HgIPMNPs and NIP nanoparticles.

Reusability and stability

The reusability and stability of HgIPMNPs for the extraction of Hg(II) was assessed by performing ten consecutive separation/desorption cycles under the optimized conditions. Desorption of Hg(II) from the adsorbent was performed with 2.0 mL of a 1:1 (v/v) mixture of thiourea (0.5 mol L^{-1})/nitric acid (0.05 mol L^{-1}) aqueous solution as described in above. There was no significant change in the performance of the adsorbent during ten cycles (Removal efficiency % = 97.2–98.6, Recovery % = 96.3–98.4), indicating that the fabricated HgIPMNPs is a reusable and stable solid-phase sorbent for the extraction of Hg(II) during this ten cycles.

Table 2 Adsorption isotherm parameters for Langmuir and Freundlich models

Isotherm model	Langmuir			Freundlich		
Parameters	K_L	q_m (mg g^{-1})	R^2	K_F	$1/n$	R^2
HgIPMNPs	0.0272	72.797	0.9900	10.1455	0.3431	0.9874
NIP	0.0308	40.145	0.9955	7.0643	0.2993	0.9678

Table 3 Assay of Hg(II) in natural and sewage water samples by means of the proposed method ($n = 3$)

Sample	Added (μg L^{-1})	Found (μg L^{-1})	RSD % ($n = 3$)	Recovery%
Tap water				
	–	ND	–	–
	50.0	51.1	2.3	102.2
	200.0	199.0	2.3	99.5
	500.0	487.0	1.9	97.4
KWC wastewater				
	–	34.0	2.6	–
	50.0	85.2	2.3	102.4
	200.0	236.0	2.2	101.0
	500.0	532.0	1.5	99.6
Radiator manufacturing wastewater				
	–	ND	–	–
	50.0	49.1	3.1	98.2
	200.0	203.0	3.1	101.5
	500.0	504.0	2.6	100.8

ND Not detected

Effect of initial sample volume

The effect of sample volume on the metal ion adsorption was studied in the range 20.0–300.0 mL. 20.0 mL samples containing 1.0 mg L^{-1} of the metal ion were diluted to 20.0, 50.0, 75.0, 100.0, 150.0, 200.0 and 300.0 mL with DDW. Then adsorption and desorption processes were performed under the optimum conditions (pH 5.5; contact time, 60 min; HgIPMNPs dosage, 0.04 g) as described in the experimental section. The results showed that the metal ion content in the volumes up to 200.0 mL was completely and quantitatively adsorbed by the nanoparticles, but there was a decrease in the amount adsorbed at higher volumes. Therefore, for the determination of trace quantities of the metal ion, a sample volume of 200.0 mL was selected for a high preconcentration factor.

Analytical parameters and applications

Calibration graph was constructed from spectrophotometric measurement of the desorbed Hg(II) after performing its adsorption/separation under the optimum conditions described above. The calibration graph was linear in the range 20.0–1,000.0 μg L^{-1} for a sample volume of 200.0 mL. The calibration equation was $A = 0.0109\ C_{Hg} + 0.0091$ with a correlation coefficient of 0.9948 ($n = 7$), where A is the absorbance of the eluate at 253.7 nm and C is the concentration of the metal ion in μg L^{-1}. The limit of detection, defined as LOD = 3 S_b/m, (where LOD, S_b and m are the limit of detection, standard deviation of the blank and the slope of the calibration graph, respectively), was 4.1 μg L^{-1} of Hg(II). As the metal ion in 200.0 mL of the sample solution was concentrated into 2.0 mL, a preconcentration factor of 100.0 was achieved in this method.

The analytical applicability of the proposed method was evaluated by determining the Hg(II) content of natural and waste water samples. The samples were also analyzed after spiking with different amounts of the Hg(II). The results given in Table 3 shows good recoveries of the proposed method for the Hg(II) added to investigated real samples.

To evaluate the selectivity of the synthesized HgIPMNPs adsorbent over NIP adsorbent, we investigated selectivity in the removal step of the proposed method. In this regard, the Hg(II) content of the spiked sample in the presence and/or absence of various contents of Cd^{2+}, Pb^{2+} and Ag^{+} ions was determined using the proposed method and by HgIPMNPs and/or NIP adsorbents. The results are shown in Table 4. The results indicated that the selective removal of Hg(II) by HgIPMNPs is responsible for overall selectivity of the proposed method in addition to the used selective detection method.

Conclusion

The preparation and characterization of MNPs coated with IIP layer of a mercaptoethylamino monomer polymerization homopolymers in the presence of Hg(II) ions as template was described. The synthesized nanoparticle have been used for selective extraction of Hg(II) ions prior to its flame atomic absorption spectrometric determination. The performance of the proposed method (detection limit and linear range) showed that this method is advantageous over previously reported methods such as thermospray flame furnace atomic absorption spectrometry [37], room temperature phosphorescence energy transfer [38], total reflection X-ray fluorescence spectrometry [39] and fluorimetry [40]. In comparison with the methods that use Hg(II) specific sample preparation methods, i.e. cold vapor atomic

Table 4 Determination of Hg(II) in the presence and/or absence of various contents of Cd^{2+}, Pb^{2+} and Ag^{+} ions using the proposed method ($n = 3$, condition: adsorbent: 0.01 g, total volume of the solution: 200.0 mL, pH: 5.5, contact time: 60.0 min, at 298 K)

Type of the adsorbent	Spiked value (mg L^{-1})				Hg(II) removal %	Hg(II) found (mg L^{-1})	Hg(II) recovery %	RSD %
	Hg^{2+}	Cd^{2+}	Pb^{2+}	Ag^{+}				
HgIPMNPs								
	2.0	–	–	–	98.6	1.98	99.0	2.4
	2.0	2.0	–	–	98.2	1.96	98.0	2.2
	2.0	4.0	–	–	97.4	1.92	96.0	2.5
	2.0	–	2.0	–	97.6	1.93	96.5	1.8
	2.0	–	4.0	–	96.5	1.90	95.0	3.1
	2.0	–	–	2.0	98.1	1.95	97.5	1.6
	2.0	–	–	4.0	97.2	1.94	97.0	2.2
NIP								
	1.0	–	–	–	98.3	0.96	96.0	3.1
	1.0	1.0	–	–	94.2	0.84	84.0	2.6
	1.0	2.0	–	–	62.3	0.41	41.0	1.9
	1.0	–	1.0	–	91.5	0.81	81.0	2.6
	1.0	–	2.0	–	53.8	0.38	38.0	1.8
	1.0	–	–	1.0	97.6	0.92	92.0	2.2
	1.0	–	–	2.0	48.0	0.29	29.0	2.2

absorption spectrometry [41–43], and more sensitive instrumental detection methods, such as ICP [44–46], the proposed method cannot provide comparable detection limit and linear range criterions. But it should be highlighted that the proposed method have some outstanding advantages over these methods such as high removal capacity, more selective extraction step, more reachable detection instruments and, to some extent, is inexpensive and more rapid.

Acknowledgments The authors acknowledge the Bu-Ali Sina University Research Council and Center of Excellence in Development of Environmentally Friendly Methods for Chemical Synthesis (CEDEFMCS) for providing support to this work.

References

1. R.B. Hayes, Cancer Cause. Control **8**, 371 (1997)
2. A. Afkhami, M. Saber-Tehrani, H. Bagheri, T. Madrakian, Microchim. Acta **172**, 125 (2011)
3. M. Saraji, H. Yousefi, J. Hazard. Mater. **167**, 1152 (2009)
4. T. Madrakian, A. Afkhami, M. Rahimi, J. Radioanal. Nucl. Chem. **292**, 597 (2012)
5. T. Madrakian, A. Afkhami, N. Rezvani-jalal, M. Ahmadi, J. Iran. Chem. Soc. **11**, 489 (2014)
6. F. Sabermahani, M.A. Taher, Microchim. Acta **159**, 117 (2007)
7. B. Godlewska-Zyłkiewicz, J. Malejko, P. Hałaburda, B. Le´sniewska, A. Kojło, Microchem. J. **85**, 314 (2007)
8. N. Rajesh, B. Deepthi, A. J. Hazard. Mater. **144**, 464 (2006)
9. E. Kenduzler, S. Baytak, O. Yalcinkaya, A.R. Türker, Can. J. Anal. Sci. Spectrosc. **52**, 91 (2007)
10. S.P. Quináia, M.C.E. Rollemberg, J.B.B. da Silva, Can. J. Anal. Sci. Spectrosc. **51**, 225 (2006)
11. K.Y. Aktas, H. Ibar, Rev. Roum. Chim. **50**, 277 (2005)
12. V.A. Lemos, E.S. Santos, E.M. Gama, Sep. Purif. Technol. **56**, 212 (2007)
13. R.S. Praveen, G.R.K. Naidu, T.P. Rao, Anal. Chim. Acta **600**, 205 (2007)
14. T. Madrakian, M. Ahmadi, A. Afkhami, M. Soleimani, Analyst **138**, 4542 (2013)
15. A. Afkhami, H. Ghaedi, T. Madrakian, M. Ahmadi, H. Mahmood-Kashani, Biosens. Bioelectron. **44**, 34 (2013)
16. S. Rimmer, Chromatographia **67**, 343 (2008)
17. D. Wang, S. Pyo, G. Hong, K. Yang, H.O. Row, Korean J. Chem. Eng. **20**, 1073 (2003)
18. I.A. Nicholls, J.P. Rosengren, Bioseparation **10**, 301 (2002)
19. B. Sellergren (ed.), *Molecularly Imprinted Polymers: Man-Made Mimics of Antibodies and Their Applications in Analytical Chemistry (Techniques and Instrumentation in Analytical Chemistry)*, vol. 23 (Elsevier, Amsterdam, 2001)
20. S.G. Dmitrienko, V.V. Irkha, A.Y. Kuznetsova, Y.A. Zolotov, J. Anal. Chem. **59**, 808 (2004)
21. Y.W. Liu, X.J. Chang, S. Wang, Anal. Chim. Acta **519**, 173 (2004)
22. Q. He, X.J. Chang, Q. Wu, X.P. Huang, Z. Hu, Y.H. Zhai, Anal. Chim. Acta **605**, 192 (2007)
23. Y.H. Zhai, Y.W. Liu, X.J. Chang, S.B. Chen, X.P. Huang, Anal. Chim. Acta **593**, 123 (2007)
24. A. Nastasovic, S. Jovanovic, D. Dordevic, D. Onjia, D. Jakovljevic, T. Novakovic, React. Funct. Polym. **58**, 139 (2004)
25. P. Tzvetkova, P. Vassileva, R. Nickolov, J. Porous Mater. **17**, 459 (2010)
26. D.L. Guerra, R.R. Viana, C. Mater, Res. Bull. **44**, 485 (2009)
27. T. Duan, J. Kang, H. Chen, X. Zeng, Spectrochim. Acta Part B **58**, 1679 (2003)
28. T. Madrakian, A. Afkhami, M. Rahimi, M. Ahmadi, M. Soleimani, Talanta **115**, 468 (2013)
29. T. Madrakian, A. Afkhami, M.A. Zolfigol, M. Ahmadi, N. Koukabi, Nano Micro Lett. **4**, 57 (2012)
30. T. Madrakian, A. Afkhami, H. Mahmood-Kashani, M. Ahmadi, Talanta **105**, 255 (2013)

31. S. Singh, K.C. Barick, D. Bahadur, J. Hazard. Mater. **192**, 1539 (2011)
32. S. Azizian, J. Colloid Interf. Sci. **276**, 47 (2004)
33. Y.T. Zhou, B.W. Christopher, H.L. Nie, Colloid Surf. B **74**, 244 (2009)
34. Y.F. Lin, H.W. Chen, P.S. Chien, C.S. Chiou, J. Hazard. Mater. **185**, 1124 (2011)
35. H. Freundlich, W. Heller, J. Am. Chem. Soc. **61**, 2228 (1939)
36. I. Langmuir, J. Am. Chem. Soc. **38**, 2221 (1916)
37. A. Gaspar, H. Berndt, Spectrochim. Acta B **55**, 587 (2000)
38. B.S.V. Riva, M. José, C.F.W.J. Jin, R. Pereiro, A. Sanz-Medel, Anal. Chim. Acta **455**, 179 (2000)
39. E. Marguía, P. Kregsamerb, M. Hidalgoc, J. Tapiasd, I. Queralta, C. Streli, Talanta **82**, 821 (2010)
40. L. Wang, L. Dong, G.R. Bian, T.T. Xia, Spectrochim. Acta A **62**, 313 (2005)
41. Y. Zhai, S.E. Duan, Q. He, X. Yang, Q. Han, Microchim. Acta **169**, 353 (2010)
42. A.M. Fernandez-Fernandez, A. Moreda-Pineiro, P. Bermejo-Barrera, J. Anal. At. Spectrom. **22**, 573 (2007)
43. N. Ferrua, S. Cerutti, J.A. Salonia, R.A. Olsina, L.D. Martinez, J. Hazard. Mater. **141**, 693 (2007)
44. L. Zhang, X. Chang, Z. Hu, L. Zhang, J. Shi, R. Gao, Microchim. Acta **168**, 79 (2010)
45. M. Faraji, Y. Yamini, M. Rezaee, Talanta **81**, 831 (2010)
46. X. Chai, X. Chang, Z. Hu, Q. He, Z. Tu, Z. Li, Talanta **82**, 1791 (2010)